Diversity Analysis of Bit-Interleaved Coded Multiple Beamforming with Orthogonal Frequency Division Multiplexing

Boyu Li and Ender Ayanoglu

Center for Pervasive Communications and Computing
Department of Electrical Engineering and Computer Science
The Henry Samueli School of Engineering
University of California - Irvine
Irvine, California 92697-2625
Email: boyul@uci.edu, ayanoglu@uci.edu

***Abstract*—For Multiple-Input Multiple-Output (MIMO) systems with frequency selective fading channels, Bit-Interleaved Coded Multiple Beamforming (BICMB) with Orthogonal Frequency Division Multiplexing (OFDM) can be employed to offer both spatial and multipath diversity, making it an important technique. Nevertheless, analyzing its diversity is a challenging problem. In this paper, the diversity analysis of BICMB-OFDM is carried out. First, the maximum achievable diversity is derived and a full diversity condition is proved. Then, the performance degradation due to the subcarrier correlation is investigated. Finally, the subcarrier grouping technique is applied to combat the performance degradation and provide multi-user compatibility.**

I. Introduction

In a MIMO system, beamforming with Singular Value Decomposition (SVD) can be employed to improve the data rate or the performance, when the channel state information is available at both the transmitter and receiver [1]. For flat fading MIMO channels, single beamforming carrying only one symbol at a time achieves full diversity [2]. However, without channel coding, multiple beamforming transmitting multiple streams simultaneously results in full diversity loss. To combat the performance degradation, BICMB which interleaves the bit codeword through multiple subchannels, was proposed [3], [4]. BICMB can achieve full diversity as long as the code rate R_c and the number of employed subchannels S satisfy the condition $R_cS \leq 1$ [5], [6]. If the MIMO channel is in frequency selective fading, BICMB can be combined with OFDM to combat the inter-symbol interference caused by multipath propagation and achieve both spatial and multipath diversity [3]. OFDM is well-suited for broadband data transmission and has been selected as the air interface for IEEE 802.11 WiFi, IEEE 802.16 WiMAX, and 3GPP LTE [7]. Although some more modern standards employ more sophisticated codes than convolutional codes employed by BICMB, such as turbo codes and LDPC codes, convolutional codes are important since they can be analyzed and there are many legacy products using them. Therefore, BICMB-OFDM is an important technique for broadband wireless communication. However, the diversity analysis of BICMB-OFDM is a difficult challenge.

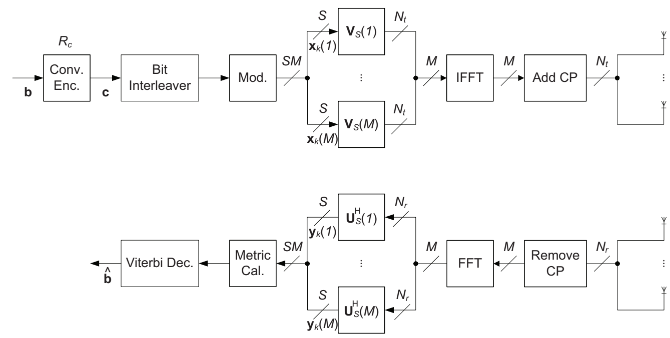

Fig. 1. Structure of BICMB-OFDM.

In this paper, diversity analysis of BICMB-OFDM is carried out. The remainder of this paper is organized as follows: In Section II, the system model is outlined. In Section III, the maximum achievable diversity is derived, and a sufficient and necessary full diversity condition $R_cSL \leq 1$ is proved where S is the number of steams transmitted at each subcarrier and L is the number of channel taps. Then, Section IV investigates the performance degradation caused by subcarrier correlation and Section V discusses the subcarrier grouping technique [8] to combat the performance degradation and provide multi-user compatibility. In Section VI, simulation results are provided. Finally, a conclusion is drawn in Section VII.

II. System Model

Fig. 1 presents the structure of BICMB-OFDM. First, the convolutional encoder with rate R_c generates the bit codeword $\mathbf{c}$ from the information bits. Then, an interleaved bit sequence is generated by a bit interleaver before being modulated to a symbol sequence. Let N_r and N_t denote the number of transmit and receive antennas respectively. Assume that M subcarriers are employed, and $S \leq \min\{N_t, N_r\}$ streams are

978-1-4673-3122-7/13/$31.00 ©2013 IEEE

carried on each subcarrier simultaneously. Hence, an $S \times 1$ vector $\mathbf{x}_k(m)$ is carried on the mth subcarrier at the kth time instant with $m = 1, \ldots, M$. The length of Cyclic Prefix (CP) is $L_{cp} \geq L$ where L is the number of channel taps.

The $N_r \times N_t$ frequency selective fading MIMO channel with L taps is assumed to be Rayleigh quasi-static and known by both the transmitter and receiver, denoted as $\breve{\mathbf{H}}(l)$ with $l = 1, \ldots, L$. Let

$$\mathbf{H}(m) = \sum_{l=1}^{L} \breve{\mathbf{H}}(l) e^{-i\frac{2\pi(m-1)\tau_l}{MT}} \quad (1)$$

denote the quasi-static flat fading MIMO channel observed at the mth subcarrier, where T is the sampling period and τ_l is the lth tap delay [9]. The beamforming matrices at the mth subcarrier are derived by SVD of $\mathbf{H}(m)$, i.e., $\mathbf{H}(m) = \mathbf{U}(m)\mathbf{\Lambda}(m)\mathbf{V}^H(m)$, where $\mathbf{U}(m)$ and $\mathbf{V}(m)$ are unitary, and $\mathbf{\Lambda}(m)$ is diagonal whose sth diagonal element, $\lambda_s(m)$, is a singular value of $\mathbf{H}(m)$, which is positive and real, in decreasing order with $s = 1, \ldots, S$. The first S columns of $\mathbf{U}(m)$ and $\mathbf{V}(m)$, i.e., $\mathbf{U}_S(m)$ and $\mathbf{V}_S(m)$, are selected as beamforming matrices at the receiver and transmitter, respectively.

The multiplications with beamforming matrices are carried out at each subcarrier before executing IFFT and adding CP at the transmitter, and after executing FFT and removing CP at the receiver, respectively. Therefore, the system input-output relation for the mth subcarrier at the kth time instant is

$$y_{s,k}(m) = \lambda_s(m) x_{s,k}(m) + n_{s,k}(m), \quad (2)$$

where $y_{s,k}(m)$ and $x_{s,k}(m)$ are the sth element of the $S \times 1$ received symbol vector $\mathbf{y}_k(m)$ and the transmitted symbol vector $\mathbf{x}_k(m)$ respectively, and $n_{s,k}(m)$ is the additive white complex Gaussian noise with zero mean and variance $N_0 = N_t/\gamma$, with γ denoting the received SNR over all the receive antennas. Note that the total transmitted power is scaled by N_t in order to make the received SNR γ.

The location of the coded bit $c_{k'}$ within the transmitted symbol is denoted as $k' \to (k, m, s, j)$, which means that $c_{k'}$ is mapped onto the jth bit position on the label of $x_{s,k}(m)$. Let χ denote the signal set of the modulation scheme, and let χ_b^j denote a subset of χ whose labels have $b \in \{0, 1\}$ at the jth bit position. By using the location information and the input-output relation in (2), the receiver calculates the Maximum Likelihood (ML) bit metrics for $c_{k'} = b$ as

$$\Delta\left[y_{s,k}(m), c_{k'}\right] = \min_{x \in \chi^j_{c_{k'}}} \left|y_{s,k}(m) - \lambda_s(m)x\right|^2. \quad (3)$$

Finally, the ML decoder applies the soft-input Viterbi decoding to find a codeword $\hat{\mathbf{c}}$ with the minimum sum weight and its corresponding information bit sequence $\hat{\mathbf{b}}$ as

$$\hat{\mathbf{c}} = \arg\min_{\mathbf{c}} \sum_{k'} \Delta\left[y_{s,k}(m), c_{k'}\right]. \quad (4)$$

III. Maximum Achievable Diversity

According to (3), the Pairwise Error Probability (PEP) of BICMB-OFDM between the transmitted bit codeword $\mathbf{c}$ and the decoded bit codeword $\hat{\mathbf{c}}$ is given in [3] as

$$\Pr\left(\mathbf{c} \to \hat{\mathbf{c}}\right) \leq \mathrm{E}\left[\frac{1}{2}\exp\left(-\frac{d_{min}^2 \sum_{k', d_H} \lambda_s^2(m)}{4N_0}\right)\right], \quad (5)$$

where d_H denotes the Hamming distance between $\mathbf{c}$ and $\hat{\mathbf{c}}$, d_{min} is the minimum Euclidean distance in the constellation, and $\sum_{k', d_H}$ stands for the summation of the d_H values related to the different bits between the bit codewords.

Define an $M \times S$ matrix $\mathbf{A}$ as an α-spectrum, whose element $\alpha_{m,s}$ denotes the number of distinct bits transmitting through the sth subchannel of the mth subcarrier for an error path, which implies $\sum_{m=1}^{M} \sum_{s=1}^{S} \alpha_{m,s} = d_H$. Let $\mathbf{a}_m^T$ denote the mth row of $\mathbf{A}$. Then (5) is rewritten as

$$\Pr\left(\mathbf{c} \to \hat{\mathbf{c}}\right) \leq \mathrm{E}\left[\prod_m \exp\left(-\frac{d_{min}^2 \sum_s \alpha_{m,s} \lambda_s^2(m)}{4N_0}\right)\right]. \quad (6)$$

In this section, the maximum achievable diversity is derived for the simplest case of no subcarrier correlation. Note that subcarrier correlation has a negative effect on the performance, which will be discussed in Section IV.

Assume that different MIMO delay spread channels are uncorrelated and have equal power, and each element of each tap is statistically independent and modeled as a complex Gaussian random variable with zero mean and variance $1/L$. Further assume that the channel taps are separated by a constant sampling time, i.e., $\tau_l = (l-1)T$ in (1). Then, the correlation in absolute value between two subcarriers is

$$\begin{aligned} \rho &= \left| \frac{\mathrm{E}\left[h_{u,v}(m) h_{u,v}^*(m')\right]}{\sqrt{\mathrm{E}\left[h_{u,v}(m) h_{u,v}^*(m)\right] \mathrm{E}\left[h_{u,v}(m') h_{u,v}^*(m')\right]}} \right| \\ &= \frac{1}{L} \left| \frac{1 - \exp[-i\frac{2\pi(m-m')L}{M}]}{1 - \exp[-i\frac{2\pi(m-m')}{M}]} \right|. \end{aligned} \quad (7)$$

Note that $\rho = 0$ when $L = M$, implying that all subcarriers are uncorrelated. Note that $\mathbf{h}_{u,v} = [h_{u,v}(0), \ldots, h_{u,v}(M)]^T$ is a complex normal random vector, where $h_{u,v}(m)$ denotes the (u,v)th element in $\mathbf{H}(m)$. Therefore, based on (7), all subcarriers are independent when $L = M$. In the following part of this section, this special case is considered. Although it is not practical, its diversity analysis provides the maximum achievable diversity for the practical case, because correlation among subcarriers for the practical case has a negative effect on performance, which will be discussed in Section IV.

Since subcarriers are independent when $L = M$, the $\mathbf{\Lambda}(m)$ matrices are independent. Hence, (6) is further rewritten as

$$\Pr\left(\mathbf{c} \to \hat{\mathbf{c}}\right) \leq \prod_m \mathrm{E}\left[\exp\left(-\frac{d_{min}^2 \sum_s \alpha_{m,s} \lambda_s^2(m)}{4N_0}\right)\right]. \quad (8)$$

For each subcarrier, the terms inside the expectation in (8) can be upper bounded by employing a theorem proved in [10]. As a result, an upper bound of PEP is given by

$$\Pr\left(\mathbf{c} \to \hat{\mathbf{c}}\right) \leq \prod_{m, \mathbf{a}_m \neq \mathbf{0}} \zeta_m \left(\frac{d_{min}^2 \alpha_{m,min}}{4N_t}\gamma\right)^{-D_m}, \quad (9)$$

with $D_m = (N_r - \delta_m + 1)(N_t - \delta_m + 1)$, where $\alpha_{m,min}$ is the minimum non-zero element in $\mathbf{a}_m$, δ_m denotes the index of the first non-zero element in $\mathbf{a}_m$, and ζ_m is a constant. Therefore, the diversity is

$$D = \sum_{m, \mathbf{a}_m \neq \mathbf{0}} D_m. \tag{10}$$

The results of (9) and (10) show that the maximum achievable diversity of BICMB-OFDM directly depends on the α-spectra because the PEP with the worst diversity dominates the performance. Note that the α-spectra are related to the bit interleaver and the trellis structure of the convolutional code, and can be derived by a similar approach to BICMB of flat fading MIMO channels presented in [5], or by computer search. An example is provided here to show the relation between the α-spectra and the diversity. Consider the parameters $N_t = N_r = S = L = M = 2$. Assume that the $R_c = 1/2$ code with generator polynomial $(5, 7)$ in octal is employed, and the bit interleaver applies simple rotation. In this case, the dominant α-spectrum is $\mathbf{A} = [0\,1;\, 2\,2]$, which implies that $\delta_1 = 2$ and $\delta_2 = 1$. Hence, $D_1 = 1$, $D_2 = 4$. Therefore, the maximum achievable diversity order is $D = D_1 + D_2 = 5$.

Based on (9) and (10), full diversity of $N_r N_t L$ [1] can be achieved if and only if all elements in the first column of $\mathbf{A}$ are non-zero, i.e., $\alpha_{m,1} \neq 0, \forall m$, for all error events. To meet the requirement, the condition $R_c SL \leq 1$ needs to be satisfied, and the proof is provided in the following.

Proof: To prove the necessity, assume that an information bit sequence $\mathbf{b}$ with JR_cSL bits is transmitted, then a bit sequence $\mathbf{c}_{m,s}$ with J bits is transmitted at the sth subchannel of the mth subcarrier. If $R_c SL > 1$, because the number of different codewords 2^{JR_cSL} is larger than the number of different bit sequences $\mathbf{c}_{m,s}$, 2^J, there always exists at least a pair of codewords with the same $\mathbf{c}_{m,s}$. Hence, the pairs of codewords with the same $\mathbf{c}_{m,1}$ cause full diversity loss.

To prove the sufficiency, a bit interleaver with simple rotation is considered. If $R_c SL \leq 1$, all the SL subchannels could be assigned to one branch of the trellis for the convolutional code. Since the trellis can be designed such that the coded bits of the first branch splitting from the zero state are all errored bits, at least one errored bit can be carried on each subchannel for all error paths, which guarantees $\alpha_{m,1} \neq 0, \forall m$ for all error events. Therefore, full diversity can be achieved.

This concludes the proof. □

The proof of the necessity above implies that when $R_c SL > 1$, there always exists an error path with no errored bits carried on the first subchannel of a subcarrier. Therefore, full diversity cannot be achieved. In this case, the bit interleaver should be designed such that consecutive coded bits are transmitted over different subchannels to provide the maximum achievable diversity, which depends on the α-spectra.

IV. Negative Effect of Subcarrier Correlation

In practice, since M is always much larger than L, subcarrier correlation exists as shown in (7). Hence, to calculate (6), the joint Probability Density Function (PDF) of $\mathbf{\Lambda}(m)\mathbf{\Lambda}^H(m)$ for all m satisfying $\mathbf{a}_m \neq \mathbf{0}$, which are eigenvalues of a set of correlated Wishart matrices [11], is required. However, this is an extremely difficult problem. The joint PDF of two correlated Wishart matrices are given in [12], [13], which is already highly complicated. To the best of our knowledge, the joint PDF of more than two correlated Wishart matrices is not available in the literature. The maximum diversity of an OFDM-MIMO system is known to be $N_r N_t L$ [1]. In our case, however, a performance degradation caused by correlation is to be expected. Because, otherwise, the diversity can exceed the full diversity, which is a contradiction. In this section, the negative effect of correlation on the performance between two subcarriers is investigated to provide an intuitive insight.

Consider an error path whose d_H distinct bits between two bit codewords are all transmitted through two correlated subcarriers with correlation ρ, which could be the practical case. Define $X = \max(N_t, N_r)$ and $Y = \min(N_t, N_r)$. Let $\mathbf{\Phi} = [\phi_1, \ldots, \phi_Y]$ and $\tilde{\mathbf{\Phi}} = [\tilde{\phi}_1, \ldots, \tilde{\phi}_Y]$ denote the ordered eigenvalues of the two correlated Wishart matrices $\mathbf{H}\mathbf{H}^H$ and $\tilde{\mathbf{H}}\tilde{\mathbf{H}}^H$, respectively. Note that $\phi_u = \lambda_u^2$. Let $\mathbf{a} = [\alpha_1, \ldots, \alpha_Y]$ and $\tilde{\mathbf{a}} = [\tilde{\alpha}_1, \ldots, \tilde{\alpha}_Y]$ denote the α-spectra of $\mathbf{\Phi}$ and $\tilde{\mathbf{\Phi}}$ respectively. Define $\mathbf{p} = [p_1, \ldots, p_W]$ and $\tilde{\mathbf{p}} = [\tilde{p}_1, \ldots, \tilde{p}_{\tilde{W}}]$ whose elements are the indices related to non-zero elements in $\mathbf{a}$ and $\tilde{\mathbf{a}}$, respectively, i.e., $\alpha_{p_w} \neq 0$ and $\alpha_{\tilde{p}_{\tilde{w}}} \neq 0$. Similarly, define $\mathbf{q} = [q_1, \ldots, q_{Y-W}]$ and $\tilde{\mathbf{q}} = [\tilde{q}_1, \ldots, \tilde{q}_{Y-\tilde{W}}]$ whose elements are the indices related to zero elements in $\mathbf{a}$ and $\tilde{\mathbf{a}}$, respectively, i.e., $\alpha_{q_w} = 0$ and $\alpha_{\tilde{q}_{\tilde{w}}} = 0$. Then, define $\mathbf{\Phi}_\mathbf{p} = [\phi_{p_1}, \ldots, \phi_{p_W}]$, $\tilde{\mathbf{\Phi}}_{\tilde{\mathbf{p}}} = [\tilde{\phi}_{\tilde{p}_1}, \ldots, \tilde{\phi}_{\tilde{p}_{\tilde{W}}}]$, $\mathbf{\Phi}_\mathbf{q} = [\phi_{q_1}, \ldots, \phi_{q_w}]$, and $\tilde{\mathbf{\Phi}}_{\tilde{\mathbf{q}}} = [\tilde{\phi}_{\tilde{q}_1}, \ldots, \tilde{\phi}_{\tilde{q}_{\tilde{w}}}]$. Hence, the PEP in (6) is written as

$$\begin{aligned}\Pr(\mathbf{c} \to \hat{\mathbf{c}}) &\leq \mathrm{E}\left\{\exp\left[-\frac{d_{min}^2 \left(\mathbf{a}^T \mathbf{\Phi} + \tilde{\mathbf{a}}^T \tilde{\mathbf{\Phi}}\right)}{4N_0}\right]\right\} \\ &\leq \mathrm{E}\left\{\exp\left[-\mu\left(\sum_{w=1}^{W} \phi_{p_w} + \sum_{\tilde{w}=1}^{\tilde{W}} \tilde{\phi}_{\tilde{p}_{\tilde{w}}}\right)\right]\right\}\end{aligned} \tag{11}$$

with $\mu = \left(d_{min}^2 \alpha_{min}\right)/(4N_0)$, where α_{min} indicates the minimum element in $\mathbf{a}$ and $\tilde{\mathbf{a}}$. To solve (11), the marginal PDF $f(\mathbf{\Phi}_\mathbf{p}, \tilde{\mathbf{\Phi}}_{\tilde{\mathbf{p}}})$ is needed by calculating

$$f(\mathbf{\Phi}_\mathbf{p}, \tilde{\mathbf{\Phi}}_{\tilde{\mathbf{p}}}) = \int \cdots \int_{\mathcal{D}_\mathbf{q}} \int \cdots \int_{\mathcal{D}_{\tilde{\mathbf{q}}}} f(\mathbf{\Phi}, \tilde{\mathbf{\Phi}})\, \mathrm{d}\mathbf{\Phi}_\mathbf{q}\, \mathrm{d}\tilde{\mathbf{\Phi}}_{\tilde{\mathbf{q}}}. \tag{12}$$

The joint PDF $f(\mathbf{\Phi}, \tilde{\mathbf{\Phi}})$ is available in [12], [13], as

$$f(\mathbf{\Phi}, \tilde{\mathbf{\Phi}}) = \exp\left[-\frac{1}{1-\rho^2} \sum_{u=1}^{Y} \left(\phi_u + \tilde{\phi}_u\right)\right] f_1(\mathbf{\Phi}, \tilde{\mathbf{\Phi}}), \tag{13}$$

with the polynomial $f_1(\mathbf{\Phi}, \tilde{\mathbf{\Phi}})$ defined as

$$\begin{aligned}f_1(\mathbf{\Phi}, \tilde{\mathbf{\Phi}}) = &[\prod_{u<v}^{Y} (\phi_u - \phi_v)(\tilde{\phi}_u - \tilde{\phi}_v)] \\ &\times \det[(\phi_u \tilde{\phi}_v)^{(X-Y)/2} I_{X-Y}(2\sqrt{\epsilon \phi_u \tilde{\phi}_v})],\end{aligned} \tag{14}$$

where $\det[h_{u,v}]$ represents the determinant of the matrix with the (u,v)th element given by $h_{u,v}$, $I_N(\cdot)$ is a modified Bessel function of order u, and $\epsilon \approx \rho^2/(1-\rho^2)^2$. Because the exponent of μ is related to the diversity, the constant appearing in the literature is ignored in (14) for brevity.

Since the eigenvalues are positive and real, $\exp(\frac{1}{1-\rho^2}\phi_u) \leq 1$ and $\exp(\frac{1}{1-\rho^2}\tilde{\phi}_u) \leq 1$ in (13). By applying $\int_0^v u^t e^{-u}\,\mathrm{d}u \leq \frac{1}{t+1}v^{t+1}$ and $\int_0^\infty u^t e^{-u}\,\mathrm{d}u = t!$ to $\mathbf{\Phi_q}$ and $\tilde{\mathbf{\Phi}}_{\tilde{\mathbf{q}}}$, the marginal PDF $f(\mathbf{\Phi_p}, \tilde{\mathbf{\Phi}}_{\tilde{\mathbf{p}}})$ in (12) is upper bounded as

$$f(\mathbf{\Phi_p}, \tilde{\mathbf{\Phi}}_{\tilde{\mathbf{p}}}) \leq \exp\left[-\frac{\left(\sum_{w=1}^{W}\phi_{p_w} + \sum_{\tilde{w}=1}^{\tilde{W}}\tilde{\phi}_{\tilde{p}_{\tilde{w}}}\right)}{1-\rho^2}\right] \times f_2(\mathbf{\Phi_p}, \tilde{\mathbf{\Phi}}_{\tilde{\mathbf{p}}}), \tag{15}$$

where $f_2(\mathbf{\Phi_p}, \tilde{\mathbf{\Phi}}_{\tilde{\mathbf{p}}})$ is a polynomial corresponding to (13). Then (11) is rewritten as

$$\Pr(\mathbf{c} \to \hat{\mathbf{c}}) \leq \int_0^\infty \int_0^{\phi_{p_1}} \cdots \int_0^{\phi_{p_{W-1}}} \int_0^\infty \int_0^{\tilde{\phi}_{\tilde{p}_1}} \cdots \int_0^{\tilde{\phi}_{\tilde{p}_{\tilde{W}-1}}} \exp\left[-\left(\mu + \frac{1}{1-\rho^2}\right)\left(\sum_{w=1}^{W}\phi_{p_w} + \sum_{\tilde{w}=1}^{\tilde{W}}\tilde{\phi}_{\tilde{p}_{\tilde{w}}}\right)\right] \times f_2(\mathbf{\Phi_p}, \tilde{\mathbf{\Phi}}_{\tilde{\mathbf{p}}})\,\mathrm{d}\mathbf{\Phi_p}\,\mathrm{d}\tilde{\mathbf{\Phi}}_{\tilde{\mathbf{p}}}. \tag{16}$$

Since $f_2(\mathbf{\Phi_p}, \tilde{\mathbf{\Phi}}_{\tilde{\mathbf{p}}})$ is a polynomial, its multivariate terms can be integrated separately, and the overall performance is dominated by the term with the worst performance. To solve (16), a theorem in [10] can be applied to integrate $\mathbf{\Phi_p}$ and $\tilde{\mathbf{\Phi}}_{\tilde{\mathbf{p}}}$ independently for each multivariate term, and the term with the smallest degree results in the smallest degree of $(\mu + \frac{1}{1-\rho^2})^{-1}$, which dominates the overall performance. Note that the smallest degree of $f_2(\mathbf{\Phi_p}, \tilde{\mathbf{\Phi}}_{\tilde{\mathbf{p}}})$ is $(X-p_1+1)(Y-p_1+1)+(X-\tilde{p}_1+1)(Y-\tilde{p}_1+1)-W-\tilde{W}$, which is proved in the Appendix. Therefore, (16) is upper bounded by

$$\Pr(\mathbf{c} \to \hat{\mathbf{c}}) \leq \zeta\left(\frac{d_{min}^2\alpha_{min}}{4N_t}\gamma + \frac{1}{1-\rho^2}\right)^{-D}, \tag{17}$$

with $D = (X-p_1+1)(Y-p_1+1)+(X-\tilde{p}_1+1)(Y-\tilde{p}_1+1)$, where ζ is a constant.

The negative effect of subcarrier correlation ρ is proved by (17). When $\gamma \to \infty$, the diversity is the same as the uncorrelated case. However, on the practical range, the performance is degraded due to the term $\frac{1}{1-\rho^2}$, which is independent of SNR. Specifically, when ρ is small, $\frac{1}{1-\rho^2}$ is also relatively small, and its effect on the performance is not significant when SNR is relatively large, and the uncorrelated case $\rho = 0$ offers the performance upper bound. On the other hand, when ρ is large, $\frac{1}{1-\rho^2}$ is also relatively large compared to SNR, then significant performance loss could be caused, depending on SNR. When $\rho = 1$, which means all errored bits are carried on one subcarrier, no multipath diversity is achieved, and the diversity equals BICMB of flat fading MIMO channels [5], [6], which is the performance lower bound. Note that the analysis in this section can also be applied to unequal power channel taps, non-constant sampling time, and other practical situations, which cause different subcarrier correlation.

V. Subcarrier Grouping

To overcome the performance loss caused by subcarrier correlation, the subcarrier grouping technique [8] is applied. Note that $\rho = 0$ in (7) when $(m-m')L/M$ is an integer. This means that although correlation exists among subcarriers for $L < M$, some subcarriers could be uncorrelated if M/L is an integer. In this case, there are $G = M/L$ groups of L uncorrelated subcarriers. As a result, the subcarrier grouping technique is applied to transmit multiple streams of bit codewords through these G different groups of uncorrelated subcarriers, instead of transmitting one stream of the bit codeword through all the correlated subcarriers. As a result, the negative effect of subcarrier correlation is completely avoided, and the maximum achievable diversity is thereby achieved. For example, consider the case of $L = 2$ and $M = 64$. Then, the gth and the $(g+32)$th subcarriers are uncorrelated for $g = 1, \ldots, 32$. The subcarrier grouping technique can transmit 32 streams of bit codewords simultaneously through the 32 groups of two uncorrelated subcarriers without performance degradation.

Compared to no subcarrier grouping, BICMB-OFDM with subcarrier grouping achieves better performance with the same transmission rate and decoding complexity. Note that the diversity analysis for $L = M$ in Section III can be applied to BICMB-OFDM with subcarrier grouping. Therefore, the full diversity condition $R_cSL \leq 1$ holds for BICMB-OFDM with subcarrier grouping. Also note that BICMB-OFDM with subcarrier grouping can be considered as Orthogonal Frequency-Division Multiple Access (OFDMA) [7] version of BICMB-OFDM. OFDMA is a multi-user version of the OFDM and it has been used in the mobility mode of WiMAX as well as the downlink of LTE. In other words, with subcarrier grouping, BICMB-OFDM can offer multi-user compatibility.

Note that (7) is derived under the assumption of equal power channel taps. When they have different power, there are no uncorrelated subcarriers in general. However, some of them could have weak correlation. Therefore, the subcarrier grouping can still be applied to combat the diversity degradation, although it now can no longer fully recover the performance because of subcarrier correlation.

VI. Simulation Results

To verify the diversity analysis, 2×2 $M = 64$ BICMB-OFDM with $L = 2$ and $L = 4$ using 4-QAM are considered for simulations. The number of employed subchannels for each subcarrier is assumed to be the same. The generator polynomials in octal for the convolutional codes with $R_c = 1/4$ and $R_c = 1/2$ are $(5,7,7,7)$, and $(5,7)$ respectively, and the codes with $R_c = 2/3$ and $R_c = 4/5$ are punctured from the $R_c = 1/2$ code [14]. Each OFDM symbol has $4\mu s$ duration, of which $0.8\mu s$ is CP and $L_{cp} = 16$. Equal and exponential power channel taps are considered. For the exponential channel model [15], the ratios of non-negligible path power to the first path power are $-7\mathrm{dB}$, the mean excess delays are $30ns$ for $L = 2$ and $65ns$ for $L = 4$, respectively. The bit interleaver

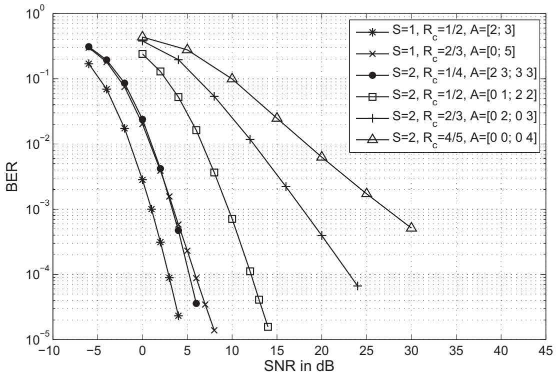

Fig. 2. BER vs. SNR for 2×2 $L = 2$ $M = 64$ BICMB-OFDM with subcarrier grouping over equal power channel taps.

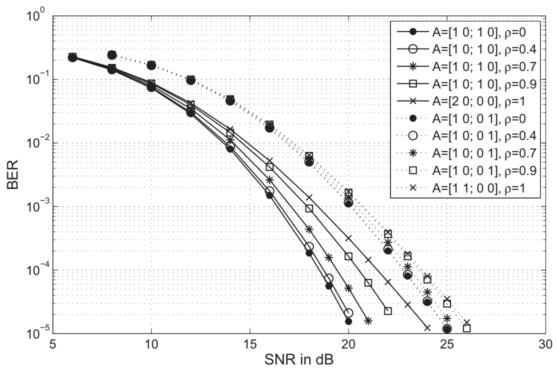

Fig. 3. BER vs. SNR for examined PEPs of two subcarriers with different correlation for 2×2 $L = 2$ $M = 64$ $S = 2$ BICMB-OFDM over equal power channel taps.

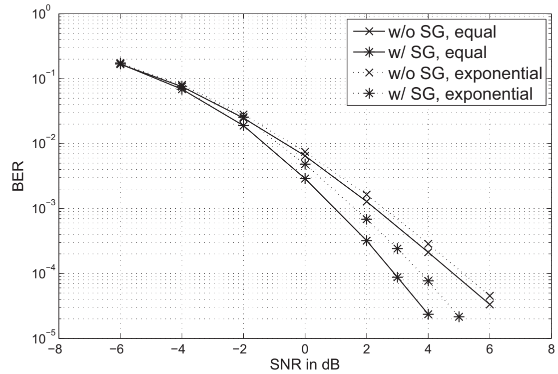

Fig. 4. BER vs. SNR for 2×2 $L = 2$ $M = 64$ $S = 1$ $R_c = 1/2$ BICMB-OFDM with and without subcarrier grouping over equal and exponential power channel taps.

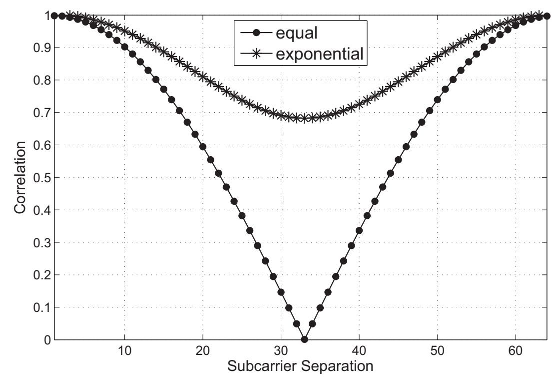

Fig. 5. Correlation vs. subcarrier separation for 2×2 $L = 2$ $M = 64$ BICMB-OFDM over equal and exponential power channel taps.

employs simple rotation. Note that although simulation results of both $L = 2$ and $L = 4$ verify our diversity analysis, only results for $L = 2$ are shown in this section because the diversity values could be investigated more explicitly through figures, and the results for $L = 4$ can be found in [16].

Fig. 2 shows the Bit Error Rate (BER) performance of BICMB-OFDM employing subcarrier grouping with different S and R_c. The $\mathbf{A}$ matrices that dominate the performance are provided in the figure. The diversity results of all curves equals the maximum achievable diversity orders derived from Section III, which is directly decided by the $\mathbf{A}$ matrices. Specifically, in the cases of $S = 1$, $R_c = 1/4$ and $R_c = 2/3$ codes achieve diversity values of 8 and 4, respectively. For $S = 2$, the codes with $R_c = 1/4$, $R_c = 1/2$, $R_c = 2/3$, and $R_c = 4/5$ offer diversity of 8, 5, 2, and 1, respectively. Note that full diversity of 8 is achieved with the condition $R_c SL \leq 1$.

Fig. 3 shows the BER performance of examined PEPs in (6) with $S = 2$, where the simplest case of an error event with $d_H = 2$ is examined for two subcarriers with different correlation coefficient ρ, which is derived from the 2×2 $L = 2$ $M = 64$ BICMB-OFDM over equal power channel taps. The figure shows that when $\rho = 0$, which implies the two subcarriers are uncorrelated, $\mathbf{A} = [1\,0; 1\,0]$ and $\mathbf{A} = [1\,0; 0\,1]$ offer diversity of 8 and 5 respectively. On the other hand, when $\rho \neq 0$, performance degradation is caused by subcarrier correlation, and stronger correlation results in worse performance loss. When $\rho = 1$, which means $d_H = 2$ distinct bits are transmitted through only one subcarrier and no multipath diversity is achieved, both $\mathbf{A} = [2\,0; 0\,0]$ and $\mathbf{A} = [1\,1; 0\,0]$ provide diversity of 4. The results are consistent with the analysis provided in Section IV, and they show the negative effect of subcarrier correlation on performance.

Fig. 4 shows the BER performance of $S = 1$ $R_c = 1/2$ BICMB-OFDM with and without subcarrier grouping over equal and exponential power channel taps. In the figure, w/ and w/o denote with and without respectively, while SG denotes subcarrier grouping. The results show that the subcarrier grouping technique can combat the performance loss caused by subcarrier correlation for both equal and exponential power channel taps. As discussed in Section V, the maximum achievable diversity of 8 is provided by employing subcarrier grouping for equal power channel taps since there is no subcarrier correlation. As for the case of exponential power channel taps, because subcarrier correlation still exists, subcarrier grouping cannot fully recover the performance loss.

Fig. 5 shows the correlation ρ of two subcarriers with different separation for equal and exponential power channel taps. The figure shows that channel with exponential power taps cause stronger subcarrier correlation than equal power taps, which results in worse performance as shown in Fig. 4.

VII. Conclusions

In this paper, the diversity analysis of BICMB-OFDM is carried out. As a result, the maximum achievable diversity is derived and a sufficient and necessary condition $R_c SL \leq 1$ for achieving full diversity is proved. In addition, the negative effect of subcarrier correlation on the performance in the practical case is investigated, and subcarrier grouping is employed to overcome the performance degradation and provide multi-user compatibility. Therefore, BICMB-OFDM can be an important technique for broadband wireless communication.

Appendix
Proof of the Smallest Degree of $f_2(\mathbf{\Phi_p}, \tilde{\mathbf{\Phi}}_{\tilde{\mathbf{p}}})$

The polynomial $f_2(\mathbf{\Phi_p}, \tilde{\mathbf{\Phi}}_{\tilde{\mathbf{p}}})$ in (15) corresponds to (13). Since $\int_0^v u^t e^{-u}\,\mathrm{d}u \leq \frac{1}{t+1}v^{t+1}$ and $\int_0^\infty u^t e^{-u}\,\mathrm{d}u = t!$, the smallest degree of $f_2(\mathbf{\Phi_p}, \tilde{\mathbf{\Phi}}_{\tilde{\mathbf{p}}})$ is related to the polynomial $f_1(\mathbf{\Phi}, \tilde{\mathbf{\Phi}})$, which is given by (14) and can be rewritten as

$$f_1(\mathbf{\Phi}, \tilde{\mathbf{\Phi}}) = \epsilon^{(X-Y)/2}[\prod_{u<v}^{Y}(\phi_u - \phi_v)(\tilde{\phi}_u - \tilde{\phi}_v)] \times [\prod_{u=1}^{Y}(\phi_u\tilde{\phi}_u)^{X-Y}]\det[\tilde{I}_{X-Y}(\epsilon\phi_u\tilde{\phi}_v)], \quad (18)$$

where $\tilde{\mathrm{I}}_N(t) = \sum_{j=0}^{\infty}\frac{t^j}{j!(j+N+1)!}$. Note that only the multivariate term of $f_1(\mathbf{\Phi}, \tilde{\mathbf{\Phi}})$ related to the smallest degree of $f_2(\mathbf{\Phi_p}, \tilde{\mathbf{\Phi}}_{\tilde{\mathbf{p}}})$ needs to be considered. Note that the dominant term of $f_1(\mathbf{\Phi}, \tilde{\mathbf{\Phi}})$ is the one with the smallest degree and the largest eigenvalues, depending on the dominant term of $\prod_{u<v}^{Y}(\phi_u - \phi_v)(\tilde{\phi}_u - \tilde{\phi}_v)$ and the dominant term of $\det[\tilde{I}_{X-Y}(\epsilon\phi_u\tilde{\phi}_v)]$. The dominant term of $\prod_{u<v}^{Y}(\phi_u - \phi_v)(\tilde{\phi}_u - \tilde{\phi}_v)$ is $\prod_{u=1}^{Y}(\phi_u\tilde{\phi}_u)^{Y-u}$. On the other hand, the dominant term of $\det[\tilde{I}_{X-Y}(\epsilon\phi_u\tilde{\phi}_v)]$ is $\zeta\prod_{u=1}^{Y}(\phi_u\tilde{\phi}_u)^{Y-u}$ with $\zeta = \prod_{u=1}^{Y}\epsilon^{Y-u}/[(Y-u)!(X-u+1)!]$ because

$$\det[\tilde{I}_{X-Y}(\epsilon\phi_u\tilde{\phi}_v)] = \sum_{u=1}^{Y}\sum_{v=1}^{Y}(-1)^{u+v} \left[\prod_{k=1}^{Y}\sum_{j_k=0}^{\infty}\frac{(\epsilon\phi_{u_k}\tilde{\phi}_{v_k})^{j_k}}{j_k!(j_k+X-Y+1)!}\right]_{j_k<j_{k+1}} \quad (19)$$

where $u_k = [(u+k-2) \bmod Y]+1$ and $v_k = [(v+k-2) \bmod Y]+1$. Hence, ignoring the constant factor, the dominant term in $f_1(\mathbf{\Phi}, \tilde{\mathbf{\Phi}})$ is given by

$$\tilde{f}_1(\mathbf{\Phi}, \tilde{\mathbf{\Phi}}) = \prod_{u=1}^{Y}(\phi_u\tilde{\phi}_u)^{X+Y-2u}. \quad (20)$$

Therefore, the degree of $\tilde{f}_1(\mathbf{\Phi}, \tilde{\mathbf{\Phi}})$ is

$$\delta_{\tilde{f}_1} = 2Y(X-1). \quad (21)$$

After integration of (12), the factor $\prod_{u=1}^{p_1-1}\phi_u^{X+Y-2u}$ and the factor $\prod_{u=1}^{\tilde{p}_1-1}\tilde{\phi}_u^{X+Y-2u}$ of $\tilde{f}_1(\mathbf{\Phi}, \tilde{\mathbf{\Phi}})$ vanish due to the fact that $\int_0^\infty u^t e^{-u}\,\mathrm{d}u = t!$. Hence,

$$\delta_{vanished} = (p_1 - 1)(X + Y - p_1) + (\tilde{p}_1 - 1)(X + Y - \tilde{p}_1). \quad (22)$$

Meanwhile, the eigenvalues ϕ_{q_u} with $q_u > p_1$ and $\phi_{\tilde{q}_u}$ with $\tilde{q}_u > \tilde{p}_1$ result in increased degree because $\int_0^v u^t e^{-u}\,\mathrm{d}u \leq \frac{1}{t+1}v^{t+1}$. Therefore,

$$\delta_{added} = 2Y - W - \tilde{W} - p_1 - \tilde{p}_1 + 2. \quad (23)$$

As a result, the smallest degree of $f_2(\mathbf{\Phi_p}, \tilde{\mathbf{\Phi}}_{\tilde{\mathbf{p}}})$ is

$$\begin{aligned}\delta &= \delta_{\tilde{f}_1} - \delta_{vanished} + \delta_{added} \\ &= (X - p_1 + 1)(Y - p_1 + 1) - W \\ &\quad + (X - \tilde{p}_1 + 1)(Y - \tilde{p}_1 + 1) - \tilde{W}. \end{aligned} \quad (24)$$

References

[1] H. Jafarkhani, *Space-Time Coding: Theory and Practice*. Cambridge University Press, 2005.

[2] E. Sengul, E. Akay, and E. Ayanoglu, "Diversity Analysis of Single and Multiple Beamforming," *IEEE Trans. Commun.*, vol. 54, no. 6, pp. 990–993, Jun. 2006.

[3] E. Akay, E. Sengul, and E. Ayanoglu, "Bit-Interleaved Coded Multiple Beamforming," *IEEE Trans. Commun.*, vol. 55, no. 9, pp. 1802–1811, Sep. 2007.

[4] E. Akay, H. J. Park, and E. Ayanoglu. (2008) On "Bit-Interleaved Coded Multiple Beamforming". arXiv: 0807.2464. [Online]. Available: http://arxiv.org

[5] H. J. Park and E. Ayanoglu, "Diversity Analysis of Bit-Interleaved Coded Multiple Beamforming," in *Proc. IEEE ICC 2009*, Dresden, Germany, Jun. 2009.

[6] ——, "Diversity Analysis of Bit-Interleaved Coded Multiple Beamforming," *IEEE Trans. Commun.*, vol. 58, no. 8, pp. 2457–2463, Aug. 2010.

[7] A. Ghosh, J. Zhang, J. G. Andrews, and R. Muhamed, *Fundamentals of LTE*. Pearson Education, Inc., 2011.

[8] Z. Liu, Y. Xin, and G. B. Giannakis, "Linear Constellation Precoding for OFDM With Maximum Multipath Diversity and Coding Gains," *IEEE Trans. Commun.*, vol. 51, no. 3, pp. 416–427, Mar. 2003.

[9] I. Lee, A. M. Chan, and C.-E. W. Sundberg, "Space-Time Bit-Interleaved Coded Modulation for OFDM Systems," *IEEE Trans. Signal Process.*, vol. 52, no. 3, pp. 820–825, Mar. 2004.

[10] H. J. Park and E. Ayanoglu, "An Upper Bound to the Marginal PDF of the Ordered Eigenvalues of Wishart Matrices and Its Application to MIMO Diversity Analysis," in *Proc. IEEE ICC 2010*, Cape Town, South Africa, May 2010.

[11] A. Edelman, "Eigenvalues and Condition Numbers of Random Matrices," Ph.D. dissertation, Massachusetts Institute of Technology, 1989.

[12] P. J. Smith and L. M. Garth, "Distribution and Characteristic Functions for Correlated Complex Wishart Matrices," *Journal of Multivariate Analysis*, vol. 98, p. 66177, Apr. 2007.

[13] P.-H. Kuo, P. J. Smith, and L. M. Garth, "Joint Density for Eigenvalues of Two Correlated Complex Wishart Matrices: Characterization of MIMO Systems," *IEEE Trans. Wireless Commun.*, vol. 6, no. 11, pp. 3902–3906, Nov. 2007.

[14] D. Haccoun and G. Begin, "High-Rate Punctured Convolutional Codes for Viterbi and Sequential Decoding," *IEEE Trans. Commun.*, vol. 37, no. 11, pp. 1113–1125, Nov. 1989.

[15] Y. S. Cho, J. Kim, W. Y. Yang, and C. G. Kang, *MIMO-OFDM Wireless Communications with MATLAB*. Wiley-IEEE Press, 2010.

[16] B. Li and E. Ayanoglu. (2011) Diversity Analysis of Bit-Interleaved Coded Multiple Beamforming with Orthogonal Frequency Division Multiplexing. arXiv: 1109.3510. [Online]. Available: http://arxiv.org